

Small-Signal Stability Analysis in an Uncertain Microgrid with Distributed Energy Resources: A Data-Driven Monitoring

Watcharakorn Pinthurat

Department of Electrical Engineering

Rajamangala University of Technology Tawan-Ok

Chanthaburi, Thailand

watcharakorn_@rmutt.ac.th

Thongchart Kerdphol

Department of Electrical Engineering

Kasetsart University,

Bangkok, Thailand

thongartkerd@gmail.com

Tossaporn Surinkaew

Department of Electrical Engineering

King Mongkut's Institute of Technology Ladkrabang

Bangkok, Thailand

tsurinkaew1@gmail.com

Boonruang Marungsri*

School of Electrical Engineering

Suranaree University of Technology

Nakhon Ratchasima, Thailand

bmshvee@sut.ac.th, *Corresponding author

Abstract—In low-inertia microgrids (MGs) with intermittent distributed energy resources (DERs), the requirement to pre-determine MG parameters results in a challenge as these parameters evolve over time. Consequently, conducting small-signal stability analysis becomes impractical due to the dynamic nature of the MG's parameter variations. In this paper, we propose an adaptive data-driven approach designed for grid-forming converters of DERs. The goal is to improve small-signal stability within a dynamically shifting window range. Additionally, we propose a data-driven approach to identify the MG model within a moving window. Subsequently, small-signal stability can be assessed. Comprehensive simulation results are systematically generated for an MG with DERs under various crucial conditions, including (i) intermittent power outputs of DERs, (ii) generator outages, (iii) diverse levels of total MG inertia, and (iv) different MG operation modes.

Index Terms—Adaptive data-driven approach, grid-forming converter, microgrid control, small-signal stability, variable inertia microgrid.

I. INTRODUCTION

Navigating the complex landscape of variable-inertia microgrids (MGs) equipped with intermittent distributed energy resources (DERs) presents a formidable challenge [1]. The need to pre-determine MG parameters is a persistent hurdle, exacerbated by their evolving nature over time. The dynamism in these parameters renders the conventional approach of conducting small-signal stability analysis impractical. As a consequence, understanding and managing the intricacies of stability in such MGs become a formidable task, requiring innovative solutions to address the inherent uncertainties and fluctuations in the MG's parameters [2], [3].

The analysis and enhancement of small-signal stability in an MG characterized by a high penetration of DERs demand an advanced approach for accurate predictions and effective

proactive measures. A data-driven methodology stands out as a superior choice compared to non-data-driven strategies, offering several key advantages that are particularly relevant in the dynamic and complex environment of modern energy systems [4], [5], [6].

The various advantages of the data-driven approach compared to the non-data-driven approach are outlined next. Literature reviews addressing challenges in MGs with DERs are provided as follows:

- In contrast to non-data-driven methods that rely on static models, a data-driven strategy continuously analyzes real-time operational data [5]. This adaptability ensures that the model remains robust in the face of changing conditions, a crucial aspect when dealing with the inherent variability and intermittency associated with DERs [7];
- One of the foremost advantages of a data-driven approach lies in its adaptability to dynamic conditions [5]. In contrast to non-data-driven methods that rely on static models, a data-driven strategy continuously analyzes real-time operational data [5] [6];
- The accuracy of stability assessments is significantly enhanced with a data-driven approach. By utilizing actual operational data, the model can more precisely capture the intricate relationships and behaviors of DERs [5], [8]. Non-data-driven approaches, relying on theoretical models, may struggle to represent the true complexity of the system, potentially leading to less accurate predictions [5], [8] [9]. The accuracy of stability assessments is significantly enhanced with a data-driven approach. By utilizing actual operational data, the model can more precisely capture the intricate relationships and behaviors of DERs;
- Crucially, a data-driven methodology excels in identify-

ing and addressing nonlinear relationships within DER behaviors. DERs often exhibit nonlinear dynamics that can have a profound impact on stability [10]. Data-driven models have the capability to capture these nonlinearities, providing a more comprehensive understanding of the system compared to non-data-driven counterparts that may oversimplify or overlook these intricate dynamics [11];

- The proactive nature of a data-driven approach is another notable advantage. This methodology is designed to proactively identify and mitigate potential stability issues [12]. It continuously learns from changing system conditions, enabling it to respond swiftly to emerging problems. In contrast, non-data-driven approaches are more reactive, potentially causing delays in issue identification and resolution. Additionally, continuous learning and adaptation are inherent to data-driven approaches [12]. In the context of an MG with high DER penetration, where the characteristics of DERs can vary significantly, this adaptability is crucial. The model learns from real-world operational patterns, optimizing its understanding of the system and ensuring efficient resource utilization [12]. Non-data-driven methods, being more static, may lead to sub-optimal resource allocation;
- Ultimately, the resilience and reliability of an MG are greatly enhanced through the real-time decision support provided by a data-driven approach. Its ability to offer timely insights and adapt to unforeseen challenges positions make it as a valuable tool in navigating the complexities of modern energy systems, particularly in MGs with high DER penetration [10], [13], [14]. In summary, the advantages of a data-driven approach underscore its significance in small-signal stability analysis and enhancement in MGs with a substantial penetration of DERs.

To facilitate the application of a data-driven approach for assessing small-signal stability of MGs with high DERs, the following contributions have been made

- We develop a data-driven approach to monitor the small-signal stability in a moving window without requiring any MG parameters and operating points. By introducing a data-driven approach for monitoring small-signal stability within a dynamic moving window, our contribution not only enhances the accuracy and efficiency of stability assessments, but also promotes adaptability to real-time changes. This methodology allows for a more responsive and proactive small-signal stability monitoring system, which enables timely identification and mitigation of potential stability issues in dynamic systems with intermittent DERs;
- We also recognize emerging critical modes associated to DERs, referred to as *DER modes*, wherein their sensitivity differs from that of conventional power systems. Here, our data-driven nature also facilitates continuous learning and adaptation, ensuring that the monitoring

system remains robust and effective in various operational conditions. This contributes to the overall resilience and reliability of the monitored systems;

- Faced with unsatisfactory small-signal stability conditions stemming from sub-optimal *DER modes*, our innovative data-driven approach can automatically detect and report these conditions. Its real-time adaptability enables swift responses, thereby providing proactive measures to promptly identify and address issues associated with DERs.

II. DYNAMICS OF LOW-INERTIA MGs

In this section, an overview of data-driven approach in variable-inertia MGs is proposed. The nonlinear equation of an MG can be represented by

$$f(\mathbf{x}(t), \mathbf{y}(t)) = 0, \quad (1)$$

where t is the moving window time, f is the nonlinear function, \mathbf{x} is the state vector, and \mathbf{y} is the output vector.

The state-space representation is frequently employed to investigate small-signal stability of systems including MGs. A fundamental state-space equation for a linear time-invariant system can be derived by linearizing (1) around an operating point at t_i , $t_i \in t$, where t_i represents the time at i -th time interval. Additionally, we assume that the system consistently encounters minor uncertainties, such as variations in parameters, large disturbances like generator/line tripping, and significant changes in system topology such as the installation or removal of MG component(s). Accordingly, Eq. (1) is equivalent to time-varying aspect [15]

$$\frac{d\mathbf{x}(t_i)}{dt} = A(t_i)\mathbf{x}(t_i) + B(t_i)\mathbf{u}(t_i), \quad (2)$$

$$\mathbf{y}(t_i) = C(t_i)\mathbf{x}(t_i) + D(t_i)\mathbf{u}(t_i), \quad (3)$$

where A , B , C , and D are respectively the state, input, output and feed-forward matrices, \mathbf{u} is the input vector or the stabilizing signal from controllers, i.e., \mathbf{K} , and \mathbf{K} is the controller matrix.

The dynamic behavior of the MG (2) can be determined through small-signal stability analysis and eigenvalues. Assuming $\mathbf{x}(t_i) = \mathbf{x}_i$, $\mathbf{u}(t_i) = \mathbf{u}_i$, $A(t_i) = A_i$, $B(t_i) = B_i$, $C(t_i) = C_i$, and $D(t_i) = D_i$, and considering the system (2) with feedback signals from \mathbf{K} , we get the relationship

$$\mathbf{u}_i = -\mathbf{K}_i \mathbf{y}_i = -\mathbf{K}_i C_i \mathbf{x}_i. \quad (4)$$

Considering (4), the matrix \mathbf{K}_i can be represented by the adaptive controller at any i -th time interval. From (4), substituting $B_i \mathbf{u}_i = -B_i \mathbf{K}_i C_i \mathbf{x}_i$, the closed-loop state matrix (denoted by $A_{cl,i}$) can be obtained as $A_{cl,i} = A_i - B_i \mathbf{K}_i C_i$. In (2), the closed-loop state vector is extended as

$$\mathbf{x}_{cl,i} = [\mathbf{x}_i \quad \mathbf{u}_i]^\top, \quad (5)$$

Accordingly, we have

$$\frac{d\mathbf{x}_{cl,i}}{dt} = \begin{bmatrix} \dot{\mathbf{x}}_i \\ \dot{\mathbf{u}}_i \end{bmatrix} = A_{cl,i} \begin{bmatrix} \mathbf{x}_i \\ \mathbf{u}_i \end{bmatrix}. \quad (6)$$

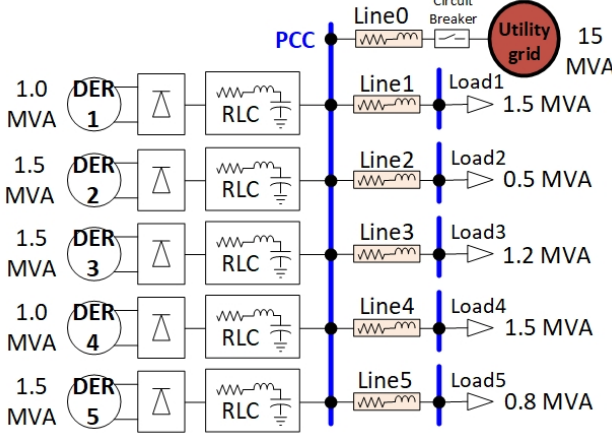


Figure 1: Test MG system with DERs (Base: 1 MVA, 60 Hz).

Let superscript $[k]$ represent the k -th column of the input matrix B_i , all elements of $A_{cl,i}$ at n -th row and m -th column (represented by the superscript $[n, m]$) are computed by

$$A_{cl,i}^{[n,m]} = A_i^{[n,m]} - \sum_{k=1}^{n_k} B_i^{[n,k]} K_i^{[k,m]} C_i^{[m,k]}, \quad (7)$$

where $k = 1, \dots, n_k$ is the counter of the vector of controller, and n_k is the total number of controllers.

Then, the eigenvalues can be computed by

$$0 = \det(A_{cl,i} - \lambda_i I), \quad (8)$$

$$\lambda_i = [\lambda_{i,1} \dots \lambda_{i,\text{length}(A_{cl,i})}], \quad (9)$$

where operator $\det(\cdot)$ means the determinant of its matrix argument, operator $\text{length}(\cdot)$ returns the length of its vector/matrix argument, I is the identity matrix, and λ_i is the vector of eigenvalues at any i -th time interval.

Solving (8), we get λ_i . Consequently, damping ratios of the system (2) (denoted by ζ_i) are computed by

$$\zeta_i = -\frac{\Re(\lambda_i)}{\sqrt{\Re(\lambda_i^2) + \Im(\lambda_i^2)}}, \quad (10)$$

where operators $\Re(\cdot)$ and $\Im(\cdot)$ return the real and imaginary parts of its vector argument.

III. DATA-DRIVEN APPROACH FOR ANALYZING SMALL-SIGNAL STABILITY

As evident from the given equations (1) – (10), it becomes apparent that comprehensive observation of all MG parameters is essential. However, the practical implementation of such an observation becomes challenging in real-world MGs, primarily due to the dynamic and intermittent nature of MGs, especially those integrated with DERs [10], [14]. The inherent variability in these parameters, coupled with the continuous changes they undergo, poses a significant obstacle to their accurate and timely measurement [13], [14]. In addressing this challenge, employing a data-driven methodology emerges as a promising approach. Leveraging data-driven methods allows for the extraction of meaningful insights from the continuously evolving parameters of MGs, providing a more adaptive and efficient

means to comprehend and manage the intricacies associated with DER integration and intermittent behavior in MGs.

For conducting the data-driven approach in the small-signal stability analysis of MGs, we selectively utilize specific output vectors y_i within our analysis. Let us express y_i in (3) in the time-domain incorporating MG oscillation modes, as described in (9) and (10), and $n_{i,j} = \text{length}(A_{cl,i})$ is the total number of eigenvalue at any i -th time interval, the measurement can observe the time-domain result

$$y_i = \sum_{j=1}^{n_{i,j}} \alpha_{i,j} \mathcal{A}_{i,j} \cos(2\pi f_{i,j}) e^{-\beta_{i,j} \zeta_{i,j}}, \quad (11)$$

where $\mathcal{A}_{i,j}$ is the oscillation amplitude at any i -th time interval corresponding to j -th eigenvalue, $f_{i,j}$ is the vector for oscillation frequencies at any i -th time interval corresponding to j -th eigenvalue, and $\alpha_{i,j}$ and $\beta_{i,j}$ are the coefficients of $\mathcal{A}_{i,j}$ and $\zeta_{i,j}$, respectively.

Here, the coefficients $\alpha_{i,j}$ and $\beta_{i,j}$ are represented by nonlinear functions associated with several factors as follows

$$\alpha_{i,j} = g_\alpha(\mathbf{x}_i, \mathbf{y}_i, \mathbf{d}_i, \dots), \quad \beta_{i,j} = g_\beta(\mathbf{x}_i, \mathbf{y}_i, \mathbf{d}_i, \dots), \quad (12)$$

where g_α and g_β are respectively the nonlinear functions associated with $\alpha_{i,j}$ and $\beta_{i,j}$, and \mathbf{d}_i is the disturbance vector at any i -th time interval.

In (11), it is established that $\alpha_{i,j} \mathcal{A}_{i,j} \propto \beta_{i,j} \zeta_{i,j}$. Describing from (11) – (12), the formulations delineate the output vector y_i as a composite of oscillations characterized by diverse amplitudes, frequencies, and decay rates. The coefficients $\alpha_{i,j}$ and $\beta_{i,j}$ control the contribution of each term in the summation. The oscillation characteristics, such as amplitude and frequency, can vary at different time intervals i and for different eigenvalues j . The determination of small-signal stability in actual MGs with DERs becomes challenging due to the necessity of acquiring and maintaining accurate values for parameters such as A_i , B_i , C_i , and D_i . This proves impractical in real MG scenarios where uncertainties and disturbances are persistent, leading to continuous fluctuations in the parameters and states of the MG over time. To address this challenge, the matrices A_i , B_i , C_i , and D_i are estimated using the subspace state-space identification method, commonly referred to as 4SID. The estimated A_i , B_i , C_i , and D_i are estimated as follows

$$A_i \approx \hat{A}_i, \quad B_i \approx \hat{B}_i, \quad C_i \approx \hat{C}_i, \quad D_i \approx \hat{D}_i, \quad (13)$$

where \hat{A}_i , \hat{B}_i , \hat{C}_i , and \hat{D}_i are the estimated A_i , B_i , C_i , and D_i by 4SID, respectively.

The matrices \hat{A}_i , \hat{B}_i , \hat{C}_i , and \hat{D}_i in Eq. (13) are ascertained through the application of the proposed data-driven method. In this approach, two output vectors are considered: (i) the average power output of DERs and conventional power plants (denoted by \bar{P}_i), and (ii) the average rate of change of

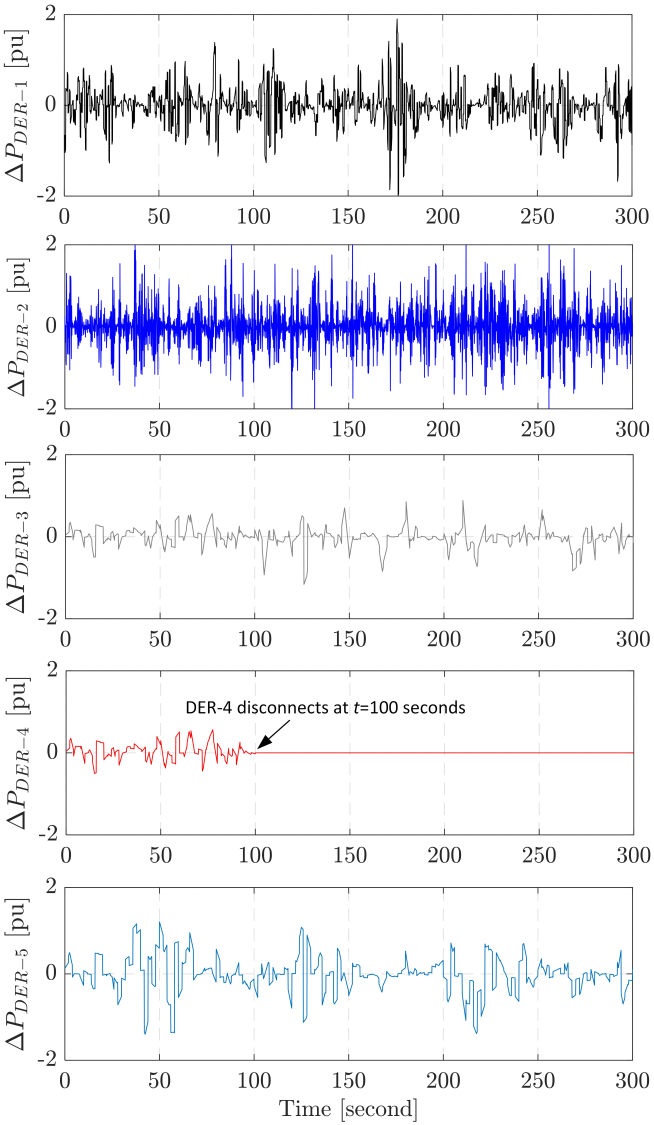


Figure 2: Active power output deviations of all DERs.

frequencies across all buses/nodes (referred to as $\text{Ro}\bar{\text{C}}\text{oF}_i$), these variables can be calculated as follows

$$IP_i = \bar{P}_i = \sum_{g=1}^{n_g} \frac{P_{i,g}}{n_g}, \quad OP_i = \text{Ro}\bar{\text{C}}\text{oF}_i = \sum_{h=1}^{n_h} \frac{\text{RoCoF}_{i,h}}{n_h}, \quad (14)$$

where IP_i and OP_i is the two input pairs at any i -th time interval used as the input of 4SID.

During each i -th time interval, we ensure the observability of all oscillation frequencies in the measured output signal. Consequently, considering a constant time stamp of Δt_s , the length of \mathbf{y}_i (denoted by $\text{length}(\mathbf{y}_i) = L_{\mathbf{y}_i}$) in second and the total number of data at any i -th time interval (denoted by $N_{\mathbf{y}_i}$) are respectively calculated by

$$L_{\mathbf{y}_i} = \frac{1}{\min(\mathbf{f}_i)}, \quad N_{\mathbf{y}_i} \geq \frac{L_{\mathbf{y}_i}}{\Delta t_s} \geq \frac{1}{\min(\mathbf{f}_i)\Delta t_s}, \quad (15)$$

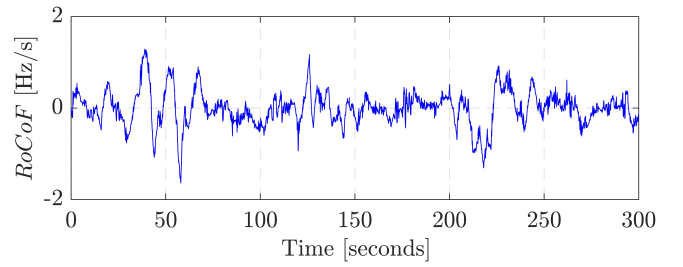


Figure 3: Mean value of RoCoF caused by active power deviations of all DERs.

Subsequently, the vector \mathbf{y}_i undergoes partitioning in a moving window by

$$\mathbf{y}_i = [\mathbf{y}_{i,1} \quad \mathbf{y}_{i,2} \quad \mathbf{y}_{i,3} \quad \dots \quad \mathbf{y}_{i,r} \quad \dots], \quad (16)$$

When $\mathbf{y}_{i,1}, \mathbf{y}_{i,2}, \mathbf{y}_{i,3}, \dots, \mathbf{y}_{i,r}$ in (16) are the 1-st, 2-nd, 3-rd, and subsequent r -th signal patterns, $r \in i$, which can be expressed by

$$\begin{aligned} \mathbf{y}_{i,1} &= [\mathbf{y}_{i,(1,1)} \quad \mathbf{y}_{i,(1,2)} \quad \mathbf{y}_{i,(1,3)} \quad \dots \quad \mathbf{y}_{i,(1,N_{\mathbf{y}_i})}], \\ \mathbf{y}_{i,2} &= [\mathbf{y}_{i,(1,2)} \quad \mathbf{y}_{i,(1,3)} \quad \mathbf{y}_{i,(1,4)} \quad \dots \quad \mathbf{y}_{i,(1,N_{\mathbf{y}_i}+1)}], \\ \mathbf{y}_{i,3} &= [\mathbf{y}_{i,(1,3)} \quad \mathbf{y}_{i,(1,4)} \quad \mathbf{y}_{i,(1,5)} \quad \dots \quad \mathbf{y}_{i,(1,N_{\mathbf{y}_i}+2)}], \\ &\vdots && \vdots \\ \mathbf{y}_{i,r} &= [\mathbf{y}_{i,(1,r)} \quad \mathbf{y}_{i,(1,r+1)} \quad \mathbf{y}_{i,(1,r+2)} \quad \dots \quad \mathbf{y}_{i,(1,N_{\mathbf{y}_i}+(r-1))}], \end{aligned} \quad (17)$$

In (16), $\mathbf{y}_{i,1}$ represents the initial data point observed within the moving window. This output vector is derived from measurements and is segmented into uniform partitions. Following the acquisition of adequate data for 4SID (specifically, $N_{\mathbf{y}_i}$), the initial data point of each pattern is subsequently omitted whenever new data is received at any subsequent time stamp Δt_s . Here, these output vectors serve as the inputs for the 4SID algorithm. Full detail of the 4SID algorithm to estimate the MG matrices is provided in [16]. As a result, the 4SID of the output signals (16) at any i -th time interval (referred to as $f_{4SID,i}$) is formulated by [16]

$$f_{4SID,i}(IP_i, OP_i) = \hat{G}_i, \quad \text{when } \hat{G}_i = \begin{bmatrix} \hat{A}_i & \hat{B}_i \\ \hat{C}_i & \hat{D}_i \end{bmatrix}, \quad (18)$$

where G_i is the system matrix at any i -th time interval.

By substituting (16) into (18), we can derive continuous values for A_i , B_i , C_i , and D_i and can consequently calculate λ_i in (8) and ζ_i in (10) at any given stamped time Δt_s . Following on, the continuous values of λ_i and ζ_i are reported in the moving window. The following section presents the results and discusses their implications.

IV. RESULTS AND DISCUSSION

The diagram of the test MG system with DERs is depicted in Fig. 1, with a system base of 1 MVA and operating at a frequency of 60 Hz. The MG system comprises five DERs with capacities ranging from 1.0 MVA to 1.5 MVA, as well as five distributed loads with capacities ranging from 0.5 MVA to 1.5 MVA. Here, the DERs are linked to their converters and RLC filters before being connected to the grid, while the lines

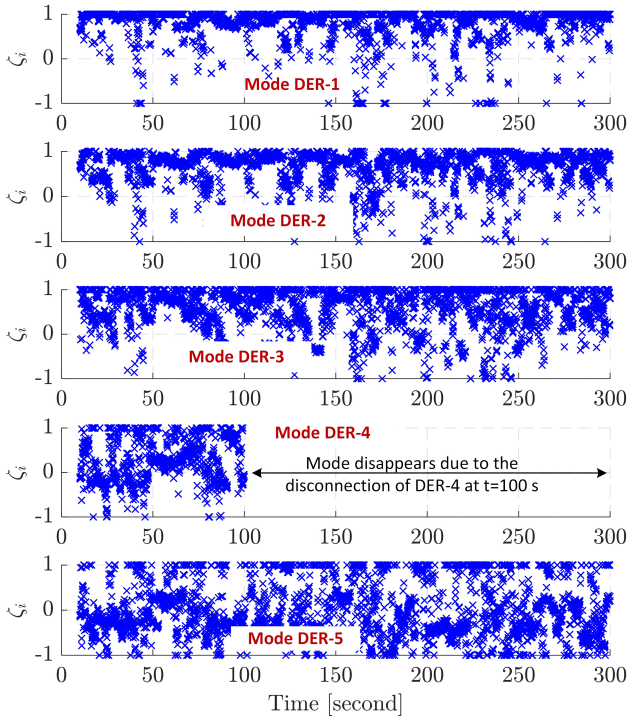


Figure 4: Small-signal stability analysis using data-driven approach with respect to i -th time interval.

are represented by RL models. The DERs produce intermittent power outputs for the MG, while the loads fluctuate within a range of -20% to +20% from their current operating points. During a normal operation, it functions in islanding mode (the circuit breaker is opened), wherein the MG is disconnected from the utility grid. In this mode, the converter of DER-2 serves as the grid-forming converter, generating reference signals for frequency and voltage, while the others operate as grid-following converters followed the reference signals generated by DER-2. As a result, Fig. 2 demonstrates the active power output deviations of all DERs during 5 minutes or 300 seconds. Specifically, it is presumed that DER-1 and DER-2 exhibit greater intermittency compared to the others, given the higher and more frequent variations in ΔP_{DER-1} and ΔP_{DER-2} . Additionally, at $t = 100$ seconds, we assume that DER-4 is disconnected from the MG, leading to the abrupt disappearance of the Mode DER-4. As a consequence, these factors contribute to the fluctuation in frequency and $RoCoF$, as illustrated in Fig. 3. Notably, the $RoCoF$ exhibits fluctuations within the defined bounds, ranging from $-1.8 \frac{\text{Hz}}{\text{s}}$ to $+1.5 \frac{\text{Hz}}{\text{s}}$. To employ a data-driven method for analyzing small-signal stability, we measure the active power outputs of all DERs depicted in Fig. 2, denoted as ΔP_{DER-1} to ΔP_{DER-5} , along with $RoCoF$ in Fig. 3. Reforming the data in Figs. 2 and 3 as expressed in (16) and (17), we can calculate the estimated \bar{A}_i , \bar{B}_i , \bar{C}_i , and \bar{D}_i by (16) – (18). Accordingly, Fig. 4 demonstrates the dynamics of ζ_i across the time domain. Concurrently, Fig. 5 displays the corresponding frequencies of the modes depicted in Fig. 4, when the frequency in Hz can be calculated by $\frac{\Im(\lambda_i)}{2\pi}$. Here, we set L_{y_i} at 10 seconds, and the

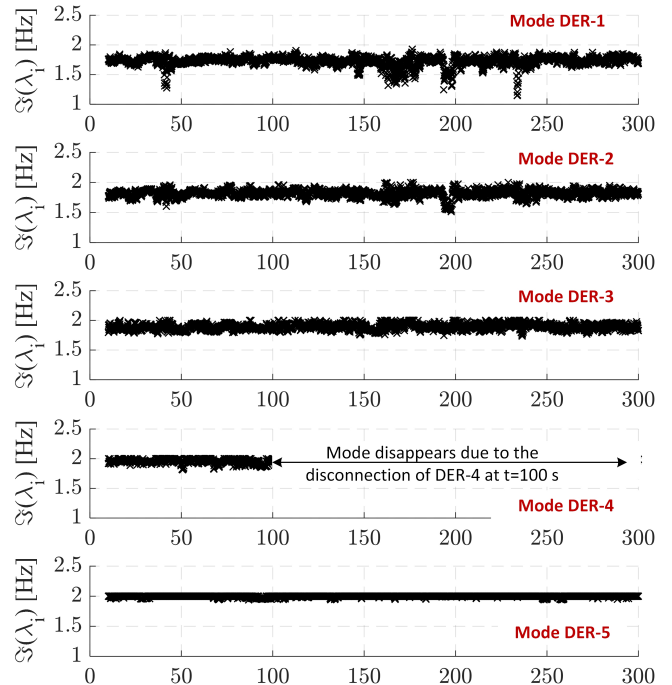


Figure 5: Oscillation frequency analysis using data-driven approach with respect to i -th time interval.

time stamp interval Δt_s to 0.1 second or 100 ms (a practical value for a phasor measurement unit). Consequently, the first result is obtained at $t = 10.1$ seconds and the moving window reports a total of $\frac{300-10}{0.1} = 2,900$ data points.

Subsequently, we employ probability analysis to assess the damping ratio ζ_i for each mode over a duration of 300 seconds. The corresponding outcome is presented in Fig. 6. The analysis suggests that Mode DER-1 and Mode DER-2 are likely to have damping ratios ζ_i consistently exceeding 50%, indicating both stable and well-damped behaviors. However, Mode DER-3 shows occasional occurrences of negative damping, which could imply instability or oscillatory behavior during certain intervals. There are instances of high damping in Mode DER-3, suggesting potential resistance to oscillations. In contrast, Mode DER-4 and Mode DER-5 consistently exhibit a very high likelihood of negative damping. This implies a persistent tendency towards unstable behavior or oscillations in these modes. The sustained high probability of negative damping in Mode DER-4 and Mode DER-5 raises concerns about the stability of the corresponding dynamic responses, suggesting a need for further investigation or mitigation strategies.

To validate the robustness of the estimated model, Fig. 7 showcases the estimation accuracy over a 300-second interval. The total data points reported in Fig. 7 align with those in Figs. 4 and 5. Notably, the presented data-driven algorithm instills confidence in the estimated model, demonstrating an accuracy surpassing 80%. This signifies that the accuracy of the estimated model exceeds the 80% threshold. As a result, this makes the proposed data-driven strategy suitable for further control and management applications. These analyses indicate that the small-signal stability in the low-inertia MG

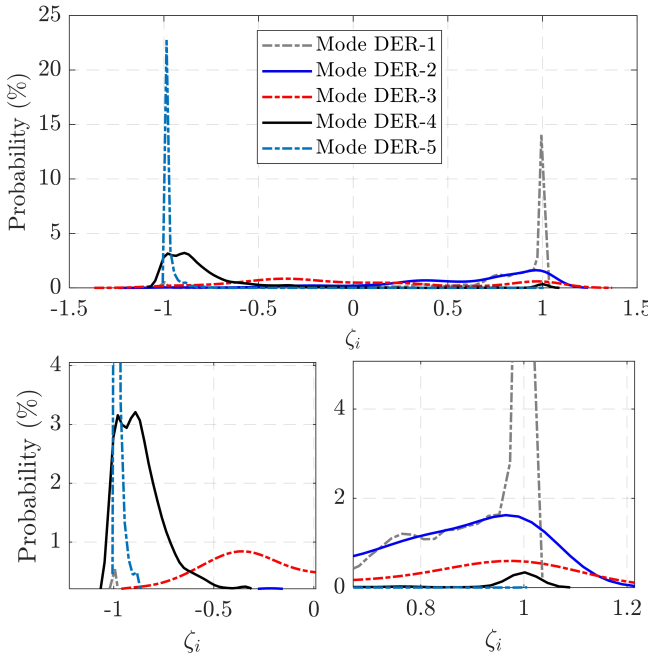


Figure 6: Probabilities of damping of all DER modes analyzed within 300 seconds.

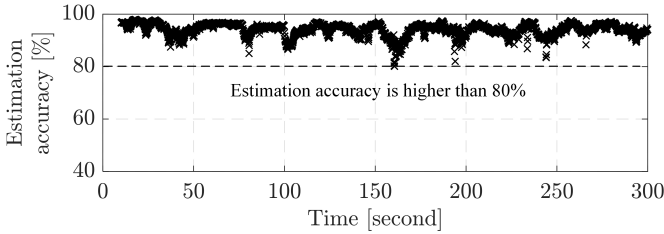


Figure 7: Estimation accuracy in percentage with respect to i -th time interval.

with DERs can be efficiently monitored and assessed using the proposed data-driven approach. The dynamic and adaptive nature of this approach allows for real-time adjustments and enhances the accuracy of stability assessments, particularly in scenarios with high DER penetration. The results demonstrate the ability of the data-driven approach to capture the complex dynamics of the system, accounting for uncertainties, variations in parameters, and intermittent behavior associated with DERs.

V. CONCLUSION

The data-driven approach presented in this paper provides a valuable tool for assessing and enhancing small-signal stability in variable inertia MGs with high DER penetration. The adaptability, accuracy, and proactive nature of the approach position make it as a promising solution for navigating the complexities of modern energy systems. As the energy landscape continues to evolve, innovative approaches like the one proposed here will play a crucial role in ensuring the stability and reliability of MGs with DERs. In addition, the proposed approach offers advantages over traditional non-data-driven methods. The adaptability to changing conditions, the ability

to capture nonlinear dynamics, and the proactive nature of the data-driven approach contribute to its effectiveness in enhancing small-signal stability in low-inertia MGs. The continuous and adaptative inherent in the data-driven approach enable it to respond swiftly to emerging challenges, providing timely insights and proactive measures for stability enhancement. For our future works, we will focus on enhancing the small-signal stability of this MG through the implementation of a data-driven approach. By employing the proposed data-driven monitoring approach, our objective is to enhance the small-signal stability of MGs with DERs in future research works.

REFERENCES

- [1] L. Lavanya and K. Swarup, "Inertia monitoring in power systems: Critical features, challenges, and framework," *Renewable and Sustainable Energy Reviews*, vol. 190, p. 114076, 2024.
- [2] J. Kweon, H. Jing, Y. Li, and V. Monga, "Small-signal stability enhancement of islanded microgrids via domain-enriched optimization," *Applied Energy*, vol. 353, p. 122172, 2024.
- [3] T. Kerdphol, I. Ngamroo, and T. Surinakew, "Forced oscillation suppression using extended virtual synchronous generator in a low-inertia microgrid," *International Journal of Electrical Power & Energy Systems*, vol. 151, p. 109126, 2023.
- [4] M. Uzair, L. Li, M. Eskandari, J. Hossain, and J. G. Zhu, "Challenges, advances and future trends in ac microgrid protection: With a focus on intelligent learning methods," *Renewable and Sustainable Energy Reviews*, vol. 178, p. 113228, 2023.
- [5] M. V. Kazemi, S. J. Sadati, and S. A. Gholamian, "Adaptive frequency control of microgrid based on fractional order control and a data-driven control with stability analysis," *IEEE Transactions on Smart Grid*, vol. 13, no. 1, pp. 381–392, 2021.
- [6] J. Wu and F. Yang, "A dual-driven predictive control for photovoltaic-diesel microgrid secondary frequency regulation," *Applied Energy*, vol. 334, p. 120652, 2023.
- [7] P. Khemmook, K. Prompinit, and T. Surinakew, "Control of a microgrid using robust data-driven-based controllers of distributed electric vehicles," *Electric Power Systems Research*, vol. 213, p. 108681, 2022.
- [8] S. S. Madani, C. Kammer, and A. Karimi, "Data-driven distributed combined primary and secondary control in microgrids," *IEEE Transactions on Control Systems Technology*, vol. 29, no. 3, pp. 1340–1347, 2020.
- [9] V. Toro, D. Tellez-Castro, E. Mojica-Nava, and N. Rakoto-Ravalontsalama, "Data-driven distributed voltage control for microgrids: A koopman-based approach," *International Journal of Electrical Power & Energy Systems*, vol. 145, p. 108636, 2023.
- [10] M. Ahmed, F. Alsokhiry, K. H. Ahmed, A. S. Abdel-Khalik, and Y. Al-Turki, "Robust damping and decoupling controller for interconnected power network based on distributed energy resources," *International Journal of Electrical Power & Energy Systems*, vol. 145, p. 108581, 2023.
- [11] M. Hasan, Z. Mifta, N. A. Salsabil, S. J. Papiya, M. Hossain, P. Roy, O. Farrok *et al.*, "A critical review on control mechanisms, supporting measures, and monitoring systems of microgrids considering large scale integration of renewable energy sources," *Energy Reports*, vol. 10, pp. 4582–4603, 2023.
- [12] L. Tightiz and J. Yoo, "A review on a data-driven microgrid management system integrating an active distribution network: Challenges, issues, and new trends," *Energies*, vol. 15, no. 22, p. 8739, 2022.
- [13] D. J. Ryan, R. Razzaghi, H. D. Torresan, A. Karimi, and B. Bahrani, "Grid-supporting battery energy storage systems in islanded microgrids: A data-driven control approach," *IEEE Transactions on Sustainable Energy*, vol. 12, no. 2, pp. 834–846, 2020.
- [14] V. Skiparev, R. Machlev, N. R. Chowdhury, Y. Levron, E. Petlenkov, and J. Belikov, "Virtual inertia control methods in islanded microgrids," *Energies*, vol. 14, no. 6, p. 1562, 2021.
- [15] I. Ngamroo and T. Surinakew, "Control of distributed converter-based resources in a zero-inertia microgrid using robust deep learning neural network," *IEEE Transactions on Smart Grid*, 2023 (Early Access).
- [16] ———, "Adaptive robust control based on system identification in microgrid considering converter controlled-based generator modes," *IEEE Access*, vol. 9, pp. 125 970–125 983, 2021.